Applied Surface Science 258 (2012) 9452–9456

Contents lists available at SciVerse ScienceDirect

Applied Surface Science

journal homepage: www.elsevier.com/locate/apsusc

Picosecond laser-induced formation of spikes in a single crystal superalloy

Wei Zhang[a,b], Guanghua Cheng[b], Qiang Feng[a,c,*], Lamei Cao[d]

[a] State Key Laboratory for Advanced Metals and Materials, University of Science and Technology Beijing, Beijing 100083, China
[b] State Key Laboratory of Transient Optics and Photonics, Xi'an Institute of Optics and Precision Mechanics of Chinese Academy of Sciences, Xi'an Shaanxi 710119, China
[c] National Center for Materials Service Safety, University of Science and Technology Beijing, Beijing 100083, China
[d] National Key Laboratory of Science and Technology on Advanced High Temperature Structural Materials, Beijing Institute of Aeronautical Materials, Beijing 100095, China

ARTICLE INFO

Article history:
Available online 19 February 2012

Keywords:
Picosecond laser
Ripples
Spikes
Capillary waves

ABSTRACT

The characteristics of laser-induced periodic surface structures (LIPSS) were investigated after laser irradiation with different pulse duration under a certain range of laser fluence ($0.25 \le \Phi \le 1.91$ J/cm^2) and pulse number ($11 \le N \le 560$). Spikes were generated by picosecond laser irradiation in ambient air, in comparison with only periodic ripple structures introduced by nanosecond and femtosecond laser irradiation. Microstructural investigations indicate that these spikes were initiated by the fragment of periodic ripple ridges or corrugation on the smooth surface with subsequent pulses, and their separation increased with increasing the laser fluence. Surface capillary waves associated with the resolidification process can be employed to explain the formation of spikes by picosecond laser irradiation.

1. Introduction

Over past decades, laser-induced periodic surface structures (LIPSS) have been investigated by using many different continuous and pulsed laser sources [1]. They can be generated in various kinds of solid materials and are attractive for potential applications in surface science and technology with submicron scale [2]. In many cases, LIPSS normally have ripple patterns and they are usually produced with single or multiple linearly polarized laser pulses [1–3]. The ripple orientation is mostly perpendicular to the polarization direction of the laser beam and its period tends to be proportional to the laser wavelength. Recently, another type of LIPSS in the appearance of spikes has been also reported in silicon by nanosecond (ns) and femtosecond (fs) laser irradiation [4–6]. And the fundamental features of spikes, such as the direction, height, size and the separation between spikes, are influenced by laser processing parameters including the state of polarization, pulse duration, laser fluence, and pulse number [4,5]. In addition, the spike formation is a dynamic iterative process related to the action of surface ablation. And each surface ablation mechanism is directly associated with laser processing parameters [6]. However, to date, fundamental mechanisms for the formation of spikes are still not well understood. Furthermore, there have been few studies on the generation of spikes in metals. In order to further understand the process and mechanism for the spike formation, detailed studies are required on the relationship among laser processing parameters, surface ablation, and spike formation.

In the current study, LIPSS on the surface of a single crystal superalloy were investigated after the irradiation by different pulsed lasers. Spikes were generated by picosecond (ps) laser ablation under a certain range of laser fluence and pulse number. Furthermore, the relationship between picosecond laser-induced periodic surface structures (ps-LIPSS) and their parametric dependence was established.

2. Experimental

A chirped pulse amplification-based Ti:sapphire regenerative amplifier laser system (Spitfire, Spectra Physics) was used to generate linearly polarized laser pulses at a center wavelength of $\lambda = 800$ nm with a maximum repetition rate of 1 kHz. Pulse durations of approximately 20 ns, 200 ps and 120 fs were obtained by adjusting the pulse compressor in the compression stage. The laser beam was perpendicular to the sample surface and focused by using a convex lens with a focal length of 120 mm. The radial direction of the laser beam was approximated by Gaussian intensity distribution. The energy of the incident laser beam was varied using a polarizer combined with a half wave plate. The sample was mounted in a computer-controlled *xyz* translation stage with a spatial resolution of 125 nm, and the experiments were carried out by translating the sample relatively to the stationary laser beam with the feedrates (ν) varying between 125 μm/s and 10,000 μm/s in

---

[*] Corresponding author at: University of Science and Technology Beijing, National Center for Materials Service Safety, 30 Xueyuan Road, Haidian District, Beijing 100083, China. Tel.: +86 10 62333584; fax: +86 10 62329915.
E-mail address: qfeng@skl.ustb.edu.cn (Q. Feng).

0169-4332/$ – see front matter © 2012 Elsevier B.V. All rights reserved.
doi:10.1016/j.apsusc.2012.02.056

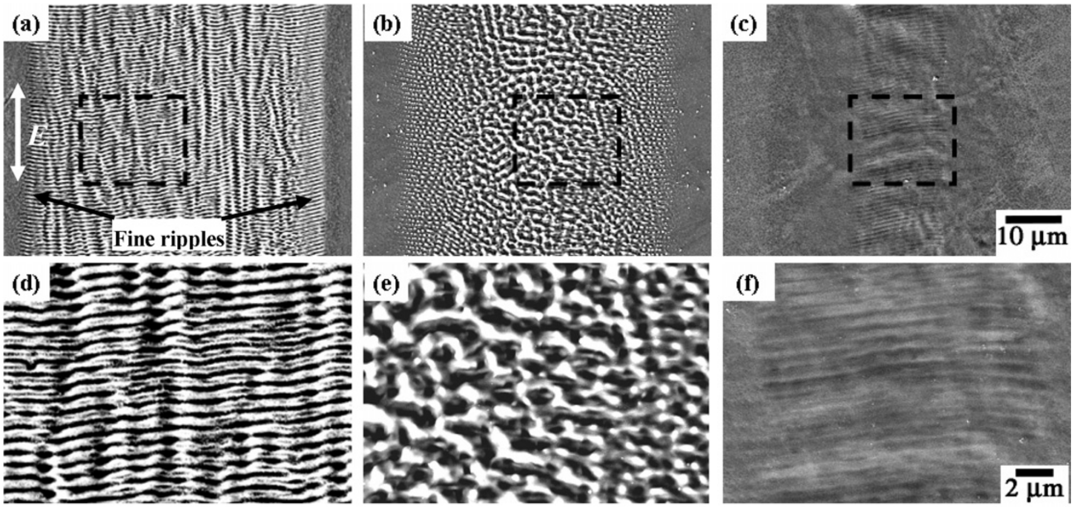

Fig. 1. Typical microstructures of LIPSS on the surface of single crystal alloy CMSX-4 at the constant laser fluence $\Phi = 0.96\,\mathrm{J/cm^2}$ and effective pulse number $N \sim 112$ after fs-, ps-, and ns-laser irradiation, respectively, (a) 120 fs, (b) 200 ps, (c) 20 ns; (d), (e) and (f) show higher magnification images of the framed area in (a), (b) and (c), respectively. *E* represents the polarization vector direction of the laser electric field.

the direction perpendicular to the incident laser beam. The corresponding effective pulse number (N) was calculated based on the feedrate and the focused beam diameter (~70 μm). All experiments were carried out in ambient air.

The sample used in the experiment was a second-generation single crystal superalloy, CMSX-4. The surface of the selected sample was polished by conventional metallographic procedures with a final polish of 0.05 μm suspended alumina powder. Before and after laser processing, the sample was subjected to ultrasonic cleaning in ethanol for 5–10 min. The morphology of the laser-induced periodic microstructure was examined by a ZEISS SUPRA 55 field-emission scanning electron microscope (FE-SEM) operated in secondary electron (SE) imaging mode. Some critical LIPSS were investigated using an Agilent Technologies 5500 atomic force microscope (AFM).

3. Results

The dependence of laser pulse duration on microstructural features was investigated in single crystal alloy CMSX-4 with various levels of laser fluence (0.25–1.91 J/cm^2) and effective pulse number (11–560). Fig. 1(a)–(c) shows the typical microstructures at the constant laser fluence $\Phi = 0.96\,\mathrm{J/cm^2}$ and the effective pulse number $N \sim 112$ after ns-, ps-, and fs-laser irradiation, respectively. Fig. 1(d)–(f) shows higher magnification images of the framed area in Fig. 1(a)–(c), respectively. After fs-laser irradiation, periodic ripples including coarse ripples in the central part and fine ripples on both sides (marked by arrows) were observed with the orientation perpendicular to the polarization of the laser beam (Fig. 1(a)). And the period of coarse ripples (~730 nm) as shown in Fig. 1(d) is close to the laser wavelength (800 nm) and two times that of fine ripples (~360 nm). These coarse ripples are also known as classical ripples [7]. When the pulse duration was 200 ps, the spike structures were fabricated as shown in Fig. 1(b) and (e). At the pulse duration of 20 ns, the irradiated surface was corrugated and periodic ripples also appeared (Fig. 1(c) and (f)) with the characteristics similar to coarse ones produced by fs-laser irradiation. It is worthy of noting that there was no sharp spike structures other than periodic ripples after ns- and fs-laser irradiation with a certain range of laser fluence (0.25–1.91 J/cm^2) and effective pulse number (11–560).

Fig. 2 is a typical AFM 3-D profile image of the spikes on the surface of single crystal alloy CMSX-4 after ps-laser irradiation with $N \sim 112$ and $\Phi = 0.96\,\mathrm{J/cm^2}$. Both the size and height of spikes were inconsistent and the base of spikes had an asymmetric shape. The average separation between spikes was determined as ~1.4 μm from the number of the spikes within an 8 μm × 8 μm square area. This value was much longer than the laser wavelength and the periodic ripple period.

The influence of the laser fluence and effective pulse number on the picosecond laser-induced spikes was also investigated. Fig. 3(a)–(c) shows the typical microstructure of the surface in single crystal alloy CMSX-4 after ps-laser irradiation at the constant laser fluence $\Phi = 0.96\,\mathrm{J/cm^2}$ with three effective pulse numbers. After the irradiation with the effective pulse number $N \sim 28$, periodic ripples were also observed as shown in Fig. 3(a) with the characteristics of classical ripples. With increasing levels of the effective pulse number, the ridges of the periodic ripples started to be rugged and subsequently fragmented into beads with the size of 100–200 nm (Fig. 3(b)). When the effective pulse number was further increased to $N \sim 80$, the periodic ripples vanished and the beads evolved into irregular spikes (Fig. 3(c)).

Fig. 4 shows another type of morphological evolution with three effective pulse numbers at higher laser fluence of 1.91 J/cm^2. At the effective pulse number of $N \sim 56$, a smooth surface with some corrugations was formed as shown in Fig. 4(a). With increasing the effective pulse number, the corrugations became sharper gradually and a unique type of spikes like pyramids was produced, where both sides and grooves of the spikes were covered with ripples

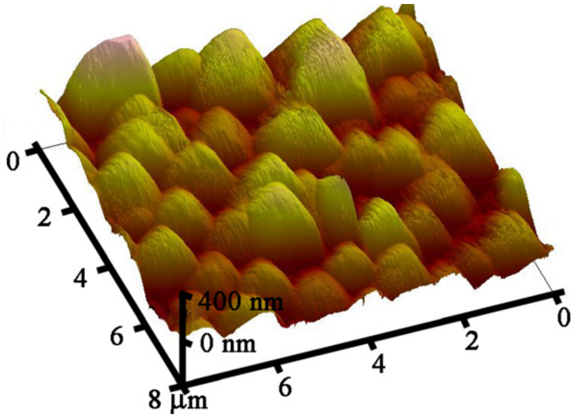

Fig. 2. AFM 3-D profile image of the surface of single crystal alloy CMSX-4 after ps-laser irradiation with $N \sim 112$ and $\Phi = 0.96\,\mathrm{J/cm^2}$.